

# A computational study of passive cooling of photovoltaic panels using hybrid material heat sink

Dang Van Binh<sup>1,2</sup>, Pham Quang Vu<sup>2</sup>, Manh-Hai Pham<sup>2</sup>

<sup>1</sup>Department of Science and Technology, Hanoi University of Industry, Hanoi, Vietnam

<sup>2</sup>Faculty of New Energy, Electric Power University, Hanoi, Vietnam

## Article Info

### Article history:

Received Dec 29, 2024

Revised Jun 6, 2025

Accepted Jul 3, 2025

### Keywords:

Conversion efficiency  
Hybrid material heat sink  
Operating temperature  
Passive cooling  
Photovoltaic panels

## ABSTRACT

Photovoltaic panels generate electricity from solar energy based on the photovoltaic effect. The conversion efficiency of photovoltaic panels depends on many factors such as solar radiation, wind speed, dust, orientation, tilt angle, and operating temperature. When the operating temperature increases by 1 °C, the conversion efficiency of photovoltaic panels decreases by 0.4% - 0.5%. Heat sink is a device used to cool electrical and electronic equipment, including photovoltaic panels. This paper presents calculating the cooling capability of hybrid heat sink made from two materials in steady state using heat transfer theory. Heat sink base is constructed from aluminum and copper layers, with copper layer thickness is 1 and 2 mm. Under different conditions of radiation intensity, wind speed, and tilt angle of photovoltaic panel, results show that heat sink added copper layers of 1 and 2 mm, the operating temperature decreases by about 0.6 K and 1.2 K compared to the aluminum base. Accordingly, the conversion efficiency of photovoltaic panel increased by 0.1% and 0.2%.

This is an open access article under the [CC BY-SA](#) license.



## Corresponding Author:

Dang Van Binh

Department of Science and Technology, Hanoi University of Industry

298 Cau Dien Street, Bac Tu Liem District, Hanoi, Vietnam

Email: binhdv@hau.edu.vn

## 1. INTRODUCTION

Through the photovoltaic effect, photovoltaic (PV) panels convert sunlight into electricity. The conversion efficiency is the ratio between the output energy (electrical energy) and the input energy (incident light energy) of PV panels. This efficiency is affected by solar radiation, wind speed, dust, direction, tilt angle, and operating temperature. For every 1°C increase in operating temperature of PV panels, the conversion efficiency decreases by 0.4% - 0.5% [1]. The amount of solar radiation converted into electricity accounts for about 6% - 20% of the total solar radiation received by PV panels [2]. The rest of the solar energy absorbed by PV panels is converted into heat, this heat increases operating temperature of PV panels [3], [4].

Cooling for PV is a solution to enhance energy efficiency and thermal management. Active and passive cooling are two techniques that reduce the temperature of PV panels. The advantages and disadvantages of these solutions are compiled from [5]–[9] and shown in Table 1. Passive cooling of PV panels is less costly, no additional energy expenditure, no operating maintenance costs or less, so passive cooling is preferred over active cooling [10].

Heat sinks made from aluminum with flat plate fins are used for passive cooling of PV panels [11]–[21]. Hernandez-Perez *et al.* [19] used plate aluminum fins with inclination for cooling of PV panels. Hernandez-Perez *et al.* [11] added discontinuous plate aluminum fins to the back of PV panel to reduce operating temperature. Heat sink with perforated aluminum fins was used to cool the PV panel, and evaluated

the cooling ability [22]–[25]. Circular aluminum is the fin shape of the heat sink used for passive cooling of monocrystalline solar panels [26], [27]. Sundarajan *et al.* [28] used copper indium gallium selenide PV panel model in Solidworks to simulate the cooling capacity of circular aluminum fins.

In addition, heat sinks made from copper have also been studied to evaluate the effectiveness of cooling photovoltaic panels [29]–[33]. Hudișteanu *et al.* [34] used copper heat sink with perforated and non-perforated fins for passive cooling of photovoltaic panels. According to the experimental results, the heat sink reduced the panel's operating temperature by 15 °C, and improved the conversion efficiency from 5.28% to 5.92%. Van Binh *et al.* [35] were compiled and evaluated the results of passive cooling solutions for PV panels using heat sinks, heat sink added to the back of PV panels can reduce the operating temperature by 7 °C - 8 °C (aluminum heat sink) and about 15 °C (copper heat sink).

Table 1. Advantages and disadvantages of cooling techniques

	Active cooling	Passive cooling
Advantages	Efficient heat transfer, precise temperature control, high cooling capacity	Good effectiveness, energy and cost saving, reliability, lifespan, quiet, environmentally friendly, easy to integrate into the system.
Disadvantages	Using external energy, complex system, environmental impact, noise, large installation space, maintenance required, operating costs	Slow heat dissipation, limited cooling capacity, difficult to temperature control.
Impact	Enhanced performance, suitable for high heat load, applicable in important field.	Energy efficiency, cost savings, low maintenance cost, environmentally friendly, natural convection, sustainable design.

Currently, heat sinks are often made from aluminum and copper. Aluminum heat sink is lightweight, cheap, but average thermal conductivity; copper heat sink has higher thermal conductivity, but heavy and expensive. Hybrid material heat sink is made from copper and aluminum; it combines the advantages of two materials to help improve heat dissipation efficiency. Nowadays, hybrid material heat sink is commonly used to cool electronic devices. For passive cooling of PV panels, most studies have focused on single material heat sink. In this study, we calculate the ability to cool PV panel using hybrid material heat sink, with aluminum fins and heat sink base is made from aluminum and copper based on heat transfer theory. The following part of the study is organized as follows: Part 2 presents calculation method; Part 3 presents parameters and data used for calculation; Results and discussion are presented Part 4. The last part is the conclusion.

## 2. CALCULATION METHOD

The PV panel adds hybrid material heat sink for passive cooling. Structural and heat transfer model shown in Figure 1. This study uses the following assumptions: i) solar radiation is stable and similar across the entire PV panel surface, ii) the surface temperature is the same in all locations, and iii) the heat flow in the system is considered steady, only allowed in one direction.

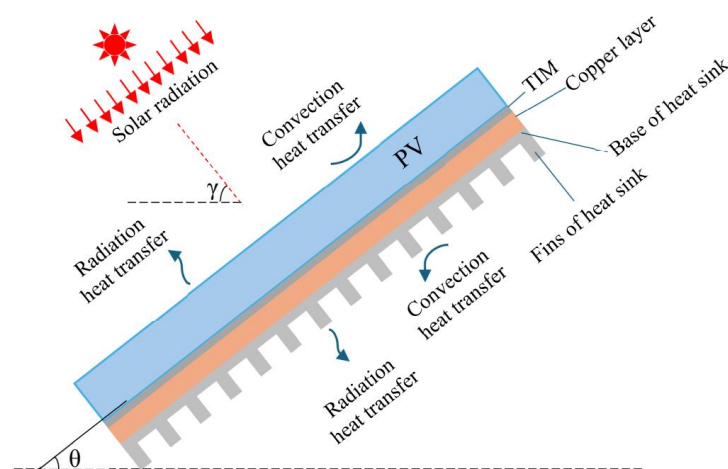


Figure 1. PV panel using hybrid material heat sink for cooling

## 2.1. Calculating the operating temperature

A part of the energy of sunlight absorbed by the PV panel will be converted into heat. This heat will be transferred to the surrounding environment through surfaces. Applying Kirchhoff's law to the thermal resistance diagram shown in Figure 2, the total heat flow transferred to the front ( $Q_1$ ) and back ( $Q_2$ ) surface of the PV panel is equal the heat flow received by the PV panel ( $Q_{solar}$ ), and expressed as (1):

$$Q_1 + Q_2 = Q_{solar} = G_{solar} \cdot A \cdot (1 - \eta) \cdot \alpha_{PV} \quad (1)$$

where  $A$ : Area of PV panel,  $m^2$ ;  $G_{solar}$ : Solar radiation,  $W/m^2$ ;  $\alpha_{PV}$ : Adsorption coefficient of PV panel;  $\eta$ : PV conversion efficiency, is determined by (2).

$$\eta = \eta_{STC} \cdot [1 - \beta \cdot (T_{PV} - T_{STC})] \quad (2)$$

where  $\eta_{STC}$ : PV conversion efficiency at STC;  $\beta$ : Temperature coefficient of PV panel at STC,  $\%/K$ ;  $T_{PV}$ : Operating temperature of PV panel, K;  $T_{STC}$ : STC temperature,  $T_{STC}=298$  K.

$$Q_1 = \frac{T_{PV} - T_a}{\sum R_f}, Q_2 = \frac{T_{PV} - T_a}{\sum R_b} \quad (3)$$

where  $\sum R_f$ : Total thermal resistance on the front side, K/W;  $\sum R_b$ : Total thermal resistance on the back side, K/W;  $T_a$ : Ambient temperature, K. From (1), (2), and (3), we obtain:

$$G_{solar} \cdot A \cdot [1 - \eta_{STC} \cdot (1 - \beta \cdot (T_{PV} - T_{STC}))] \cdot \alpha_{PV} - (T_{PV} - T_a) \cdot \frac{\sum R_f + \sum R_b}{\sum R_f \cdot \sum R_b} = 0 \quad (4)$$

where  $T_{PV}$  is the solution of (4), to determine  $T_{PV}$  we need to calculate  $\sum R_f$  and  $\sum R_b$ .  $\sum R_f$  and  $\sum R_b$  depends on  $T_{PV}$ .

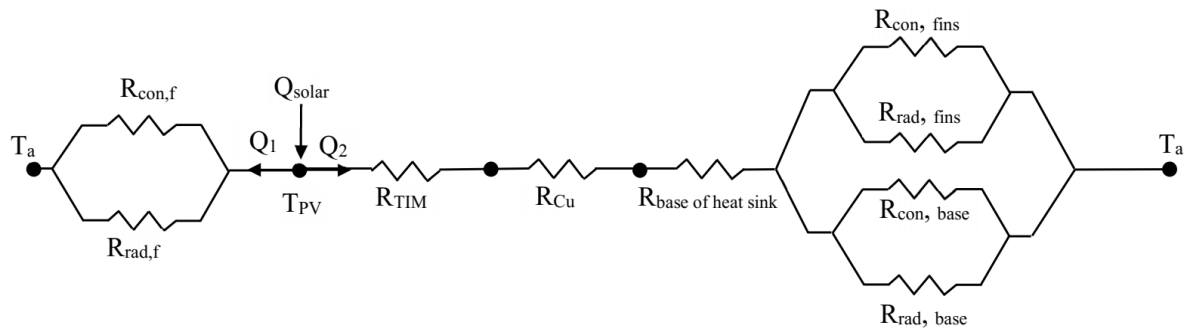


Figure 2. Diagram of thermal resistance

## 2.2. Determine the total thermal resistance on the front side

$\sum R_f$  is determined by (5):

$$\sum R_f = \frac{R_{con,f} \cdot R_{rad,f}}{R_{con,f} + R_{rad,f}} \quad (5)$$

where  $R_{con,f}$ : Thermal resistance convection on the front surface, K/W;  $R_{rad,f}$ : Thermal resistance radiation on the front surface, K/W.

$R_{rad,f}$  is determined by (6) [36]:

$$R_{rad,f} = \frac{1}{h_{rad,f} \cdot A} = \frac{1}{\varepsilon_{PV} \cdot \sigma \cdot (T_{PV}^2 + T_a) \cdot (T_{PV} + T_a)} \quad (6)$$

where  $h_{rad,f}$ : Radiation heat transfer coefficient on the front surface,  $W/m^2 \cdot K$ ;  $\varepsilon_{PV}$ : Emissivity coefficient of the front surface of PV panel;  $\sigma$ : Stefan-Boltzmann constant,  $\sigma=5.67 \times 10^{-8} W/m^2 \cdot K^4$ .

$R_{con,f}$  is determined by (7) [36], [37]:

$$R_{con,f} = \frac{1}{h_{con,f} \cdot A} = \frac{1}{\sqrt[3]{h_{con,f,f}^3 + h_{con,f,n}^3} \cdot A} \quad (7)$$

where  $h_{con,f}$ : Convection heat transfer coefficient on the front surface, W/m<sup>2</sup>.K;  $h_{con,f,f}$ ,  $h_{con,f,n}$ : Heat transfer coefficient of forced and natural convection on the front surface, K/W.  $h_{con,f,f}$  is determined according to (8) [38]:

$$h_{con,f,f} = \begin{cases} 5.74V^{0.8}L^{-0.2} & (\text{fully turbulent flow}) \\ 5.74V^{0.8}L^{-0.2} - 16.46L^{-1} & (\text{mixed flows}) \\ 3.83V^{0.5}L^{-0.5} & (\text{laminar flow}) \end{cases} \quad (8)$$

where  $V$ : Wind speed, m/s;  $L$ : PV panel length, m.  $h_{con,f,n}$  is determined according to (9) [36]:

$$h_{con,f,n} = \frac{Nu_{f,n} \cdot k_{air}}{L} \quad (9)$$

where  $k_{air}$ : Air thermal conductivity (W/m.K);  $Nu_{f,n}$ : Nusselt number of the font surface, and it is determined by (10) [39]:

$$Nu_{f,n} = \begin{cases} 0.13 \left[ (GrPr)^{\frac{1}{3}} - (Gr_c Pr)^{\frac{1}{3}} \right] + 0.56 (Gr_c Pr \sin \theta)^{\frac{1}{4}} & \text{if } \theta > 30^\circ \\ 0.13 Ra^{\frac{1}{3}} & \text{if } \theta \leq 30^\circ \end{cases} \quad (10)$$

where  $Gr$ : Grashof number;  $Pr$ : Prandtl number;  $Gr_c$ : Critical Grashof number is determined by (11):

$$Gr_c = 1.327 \times 10^{10} \exp \left[ -3.708 \left( \frac{\pi}{2} - \theta \right) \right] \quad (11)$$

where  $Ra$ : Rayleigh number, it is determined by (12) for both the front and back surfaces of the PV panel.

$$Ra = \frac{g(T_{avg} - T_a)L^3}{(0.25T_{avg} + 0.75T_a)\nu\alpha} \quad (12)$$

where  $T_{avg}$ : Average temperature of PV panel and environment, K;  $g$ : Gravity acceleration,  $g=9.81 \text{ m}^2/\text{s}$ ;  $\nu$ : Air kinematic viscosity, m<sup>2</sup>/s;  $\alpha$ : Air thermal diffusivity, m<sup>2</sup>/s.

### 2.3. Determine the total thermal resistance on the back side

$$\sum R_b = R_{TIM} + R_{Cu} + R_{bhs} + \frac{R_{base} R_{fins}}{R_{base} + R_{fins}} \quad (13)$$

where  $R_{TIM}$ : Thermal resistance of thermal interface material (TIM), K/W;  $R_{Cu}$ : Thermal resistance of copper layer, K/W;  $R_{bhs}$ : Thermal resistance of heat sink base, K/W;  $R_{base}$ : Convection and radiation thermal resistance of the base of fin, K/W;  $R_{fins}$ : Convection and radiation thermal resistance of fins, K/W;

$$R_{TIM} = \frac{\delta_{TIM}}{k_{TIM} \cdot A_{TIM}}; R_{Cu} = \frac{\delta_{Cu}}{k_{Cu} \cdot A_{Cu}}; R_{bhs} = \frac{\delta_{bhs}}{k_{bhs} \cdot A_{bhs}} \quad (14)$$

where  $\delta_{TIM}$ ,  $\delta_{Cu}$ ,  $\delta_{bhs}$ : Thickness of TIM, copper layer, heat sink base, m;  $k_{TIM}$ ,  $k_{Cu}$ ,  $k_{bhs}$ : Thermal conductivity of TIM, copper, heat sink base, W/m.K;  $A_{TIM}$ ,  $A_{Cu}$ ,  $A_{bhs}$ : Area of TIM, copper layer, heat sink base, m<sup>2</sup>.

$$R_{base} = \frac{R_{rad,base} \cdot R_{con,base}}{R_{rad,base} + R_{con,base}} \quad (15)$$

where  $R_{rad,base}$ : Thermal resistance radiation of the base of fin, K/W;  $R_{con,base}$ : Thermal resistance convection (forced and natural) of the base of fin, K/W.

$$R_{rad,base} = \frac{1}{h_{rad,base} \cdot A_{base}} \quad (16)$$

where  $h_{rad,base}$ : Radiation heat transfer coefficient of the base of fin, W/m<sup>2</sup>.K;  $A_{base}$ : Area of the base of fin, m<sup>2</sup>.

$$A_{base} = (L \times W_{hs}) - (N \times L \times \delta_{fin}) \quad (17)$$

where  $W_{hs}$ : Width of heat sink, m;  $N$ : Number of fins;  $\delta_{fin}$ : Fin thickness, m.

$h_{rad,base}$  is determined by (18) [17], [37]:

$$h_{rad,base} = \varepsilon_{base} \sigma (T_{base}^2 + T_a^2) (T_{base} + T_a) (1 - 2F_{base-fin}) \approx 4\varepsilon_{base} \sigma T_a^3 (1 - 2F_{base-fin}) \quad (18)$$

where  $\varepsilon_{base}$ : Emissivity of the base material;  $F_{base-fin}$ : View factor of the base and fin of heat sink, and it is determined according to (19):

$$F_{base-fin} = \frac{1}{\pi W} \left\{ W \tan^{-1} \frac{1}{W} + H \tan^{-1} \frac{1}{H} - (H^2 + W^2)^{\frac{1}{2}} \tan^{-1} \frac{1}{(H^2 + W^2)^{\frac{1}{2}}} \right. \\ \left. + \frac{1}{4} \ln \left[ \frac{(1+W^2)(1+H^2)}{1+W^2+H^2} \cdot \left( \frac{W^2(1+W^2+H^2)}{(1+W^2)(W^2+H^2)} \right)^{W^2} \cdot \left( \frac{H^2(1+W^2+H^2)}{(1+H^2)(W^2+H^2)} \right)^{H^2} \right] \right\} \quad (19)$$

where  $W = \frac{a_{fin}}{L}$ ;  $H = \frac{H_{fin}}{L}$  with  $a_{fin}$ : Fin spacing, m;  $H_{fin}$ : Fin height, m.

$$R_{con,base} = \frac{1}{h_{con,b} \cdot A_{base}} \quad (20)$$

where  $h_{con,b}$ : Convection heat transfer coefficient of heat sink, W/m<sup>2</sup>.K.

Convection heat transfer coefficient is combined natural and forced convection, is determined according to (21) [37]:

$$h_{con,b} = \sqrt[3]{h_{con,b,n}^3 + h_{con,b,f}^3} \quad (21)$$

where,  $h_{con,b,f}$ : Forced convection heat transfer coefficient of heat sink, is determined by (10).  $h_{con,b,n}$ : Natural convection heat transfer coefficient of heat sink, is determined according to (22) [17]:

$$h_{con,b,n} = \frac{0.02772 \times Nu_{b,n}}{L} \quad (22)$$

$Nu_{b,n}$  of the back surface of PV panel, is determined as (23) [39]:

$$Nu_{b,n} = \begin{cases} 0.58(Ra \cdot \sin \theta)^{\frac{1}{4}} & \text{if } \theta > 2^\circ \\ 0.58Ra^{\frac{1}{5}} & \text{if } \theta \leq 2^\circ \end{cases} \quad (23)$$

$$R_{fins} = \frac{R_{rad,fins} \cdot R_{con,fins}}{R_{rad,fins} + R_{con,fins}} \quad (24)$$

where  $R_{rad,fins}$ : Thermal resistance radiation of fin, K/W;  $R_{con,fins}$ : Thermal resistance convection (forced and natural) of fin, K/W.

$$R_{rad,fins} = \frac{1}{h_{rad,fins} \cdot N \cdot A_{fin}} \quad (25)$$

where  $h_{rad,fins}$ : Radiation heat transfer coefficient of fin, W/m<sup>2</sup>.K;  $A_{fin}$ : Area of a fin, m<sup>2</sup>.

$$A_{fin} = 2L \times \left( H_{fin} + \frac{\delta_{fin}}{2} \right) \quad (26)$$

$h_{rad,fin}$  is determined according to the (27) [17], [37]:

$$h_{rad,fin} = \varepsilon_{fin} \sigma (T_{fin}^2 + T_a^2) (T_{fin} + T_a) (1 - F_{fin-fin} - F_{fin-base}) \approx 4\varepsilon_{fin} \sigma T_a^3 (1 - F_{fin-fin} - F_{fin-base}) \quad (27)$$

where  $\varepsilon_{fin}$ : Emissivity of the fin material;  $F_{fin-base}$ : View factor of the fin and base of heat sink, is determined by (28):

$$F_{fin-base} = \frac{1}{\pi W'} \left\{ W' \tan^{-1} \frac{1}{W'} + H' \tan^{-1} \frac{1}{H'} - (H'^2 + W'^2)^{\frac{1}{2}} \tan^{-1} \frac{1}{(H'^2 + W'^2)^{\frac{1}{2}}} \right. \\ \left. + \frac{1}{4} \ln \left[ \frac{(1+W'^2)(1+H'^2)}{1+W'^2+H'^2} \cdot \left( \frac{W'^2(1+W'^2+H'^2)}{(1+W'^2)(W'^2+H'^2)} \right)^{W'^2} \cdot \left( \frac{H'^2(1+W'^2+H'^2)}{(1+H'^2)(W'^2+H'^2)} \right)^{H'^2} \right] \right\} \quad (28)$$

where  $W' = \frac{H_{fin}}{L}$ ;  $H' = \frac{a_{fin}}{L}$

$F_{fin-fin}$ : View factor of the fin and fin of heat sink, is determined by (29):

$$F_{fin-fin} = \frac{2}{\pi XY} \left\{ \ln \left[ \frac{(1+X^2)(1+Y^2)}{1+X^2+Y^2} \right]^{\frac{1}{2}} + X(1+Y^2)^{\frac{1}{2}} \tan^{-1} \frac{X}{(1+Y^2)^{\frac{1}{2}}} \right. \\ \left. + Y(1+X^2)^{\frac{1}{2}} \tan^{-1} \frac{Y}{(1+X^2)^{\frac{1}{2}}} - X \tan^{-1} X - Y \tan^{-1} Y \right\} \quad (29)$$

where  $X = \frac{L}{a_{fin}}$ ;  $H' = \frac{H_{fin}}{a_{fin}}$

$$R_{con,fin} = \frac{1}{h_{con,b,n} \eta_{fin} A_{fin}} \quad (30)$$

where  $\eta_{fin}$ : Fin efficiency, and it is determined according to (31) [37]:

$$\eta_{fin} = \frac{\tanh m(L + \frac{\delta_{fin}}{2})}{m(L + \frac{\delta_{fin}}{2})} \quad (31)$$

with  $m$  is constant,  $m = \sqrt{\frac{2h_{con,b}}{k_{fin}\delta_{fin}}}$

PV panel does not add heat sink, the total thermal resistance on the back side is determined as (32):

$$\sum R_b = \frac{R_{con,b} R_{rad,b}}{R_{con,b} + R_{rad,b}} \quad (32)$$

where  $R_{con,b}$ : Thermal resistance convection of back side, K/W;  $R_{rad,b}$ : Thermal resistance radiation of back side, K/W.

Thermal resistance radiation of back side is determined as (6). Thermal resistance convection of back side is determined by (33) [36], [37]:

$$R_{con,b} = \frac{1}{\sqrt[3]{h_{con,b,f}^3 + h_{con,b,n}^3} A} \quad (33)$$

where  $h_{con,b,f}$ ,  $h_{con,b,n}$ : Forced and natural convection heat transfer coefficient of back surface of PV panel and surrounding environment, K/W.  $h_{con,b,f}$  is determined as (8),  $h_{con,b,n}$  is determined as (22).

### 3. PARAMETERS AND CALCULATION DATA

Table 2 shows basic parameters of PV panel and heat sink. TIM is used to connect heat sink to PV panel, and it has thickness  $\delta_{TIM} = 1$  mm, thermal conductivity  $k_{TIM} = 1.5$  W/m.K. The environmental conditions used for calculation are the ambient temperature at certain times on 27 April 2024 in Hanoi (the hottest day of 2024 in Hanoi), as shown in Table 3. The calculations use data from the Vietnam Meteorological and Hydrological Administration, Ministry of Agriculture and Rural Development, Vietnam.

Table 2. Parameters of PV panel and heat sink

No.	Parameters	Value	No.	Parameters	Value
I	PV panel		II	Heat sink	
I.1	Maximum power, $P_{\max}$	50 W	II.1	Material (fin and base)	Aluminum, Copper
I.2	Cell type	Monocrystalline	II.2	Dimensions (L×W)	710×540 mm
I.3	No. of cell	18	II.3	Fin height, $H_{\text{fin}}$	15 mm
I.4	Dimensions (L×W×H)	710×540×30 mm	II.4	Fin thickness, $\delta_{\text{fin}}$	1.5 mm
I.5	Efficiency, $\eta$	16.8%	II.5	Fin spacing, $a_{\text{fin}}$	4.5 mm
I.6	Temperature coefficients of $P_{\max}$ , $\beta$	-0.38%/K	II.6	Base thickness (copper and aluminum layers)	3 mm
I.7	Emissivity, $\epsilon_{\text{PV}}$	0.91	II.7	Number of fins	90
I.8	Adsorption, $\alpha_{\text{PV}}$	0.96	II.8	Aluminum thermal conductivity	205 W/m.K
			II.9	Copper thermal conductivity	380 W/m.K
			II.10	Emissivity of aluminum	0.05

Table 3. Ambient temperature on 27 April 2024 in Hanoi (Unit: °C)

No.	Time	Temperature
1	07h00	28
2	09h00	31
3	11h00	35
4	13h00	38
5	15h00	40
6	17h00	37

#### 4. RESULTS AND DISCUSSION

We calculated the operating temperature of PV panel with the parameters and environmental conditions in section 3 with the following cases:

Case 1: PV panel without cooling

Case 2: PV panel is cooled by aluminum heat sink (thickness of aluminum base: 3 mm)

Case 3: PV panel is cooled by heat sink, with base consisting of 2 layers (copper: 1 mm and aluminum: 2 mm).

Case 4: PV panel is cooled by heat sink, with base consisting of 2 layers (copper: 2 mm and aluminum: 1 mm).

##### 4.1. Operating temperature at solar radiation levels

The operating temperature was calculated with wind speed of  $v=2$  m/s, tilt angle  $\theta=15^\circ$ , and solar radiation of 600, 800, and 1000 W/m<sup>2</sup>. The results are shown in Figure 3. The operating temperature of PV panel cooled by heat sink is lower than PV panel without cooling. At solar radiation of 600 W/m<sup>2</sup>, the average operating temperature for Case 1 is 329.2 K; for Case 2 is 324.2 K, reduced by 5 K; for Case 3 is 323.6 K, reduced by 5.6 K; and for Case 4 is 323.0 K, reduced by 6.2 K in Figure 3(a). At solar radiation of 800 W/m<sup>2</sup>, the average operating temperature for Cases 2, 3, and 4 are 336.5, 329.7, 329.1, and 328.5 K, respectively, reduced by 6.8, 7.4, and 8 K compared to without cooling in Figure 3(b). At solar radiation of 1000 W/m<sup>2</sup>, the average operating temperature for Cases 2, 3, and 4 are 335.2, 334.6, and 334.0 K, respectively, reduced by 8.7, 9.3, and 9.9 K compared to Case 1 in Figure 3(c). This result is quite similar to the simulation results in research [40].

Figure 4 shows the efficiency of PV panel at solar radiation levels with and without cooling. PV panel without cooling (Case 1), the efficiency is 14.8% (at 600 W/m<sup>2</sup>), 14.3% (at 800 W/m<sup>2</sup>), and 13.9% (at 1000 W/m<sup>2</sup>). In Case 2, the efficiency is 15.1% (at 600 W/m<sup>2</sup>), 14.8% (at 800 W/m<sup>2</sup>), and 14.4% (at 1000 W/m<sup>2</sup>). In Case 3, the efficiency is 15.2% (at 600 W/m<sup>2</sup>), 14.9% (at 800 W/m<sup>2</sup>), and 14.5% (at 1000 W/m<sup>2</sup>). All levels of solar radiation, the efficiency for Case 4 is 0.1 higher than Case 3.

##### 4.2. Operating temperature at different wind speeds

The operating temperature was measured with solar radiation of 800 W/m<sup>2</sup>, tilt angle  $\theta=15^\circ$ , and wind speeds of 0, 1, 2, 3, 4, and 5 m/s. The result is presented in Figure 5. When wind speed increases, the heat transfer coefficient between PV panel, heat sink, and the environment also increases, resulting in better cooling for PV panel. At wind speed of 0 m/s, the operating temperature decreased by 22 K (Case 2), 22.6 K (Case 3), and 23.2 K (Case 4) compared to Case 1 in Figure 5(a). At wind speed of 1 m/s, the operating temperature decreased by 13.6 K (Case 2), 14.2 K (Case 3), and 14.8 K (Case 4) compared to Case 1 in Figure 5(b). At wind speed of 2 m/s, the operating temperature decreased by 6.8 K (Case 2), 7.4 K (Case 3), and 8 K (Case 4) compared to Case 1 in Figure 5(c). At wind speed of 3 m/s, the operating temperature reduced by 4.3 K (Case 2), 4.9 K (Case 3) and 5.5 K (Case 4) compared to Case 1 in Figure 5(d). At wind speed of 4 m/s, the operating temperature decreased by 3 K (Case 2), 3.6 K (Case 3) and 4.2 K (Case 4) compared to Case 1 in Figure 5(e). At wind speed of 5 m/s, the operating temperature decreased by 2.3 K (Case 2), 2.9 K (Case 3) and 3.5 K (Case 4) compared to Case 1 in Figure 5(f). Calculation results confirm

that as the wind speed increases, the operating temperature of the PV panel decreases. However, with high wind speed, the cooling efficiency of the heat sink is not much higher than without cooling.

Figure 6 presents the efficiency of PV panel at different wind speeds with and without cooling by heat sink. At wind speeds of 0, 1, 2 m/s, the efficiency of PV panel with cooling (Cases 2, 3, 4) increases significantly compared to without cooling (Case 1). However, at wind speeds of 3, 4, 5 m/s, the efficiency of PV panel with and without cooling is not much different, because the operating temperature is not too different.

#### 4.3. Operating temperature at different tilt angles

We calculate the operating temperature with solar radiation of  $800 \text{ W/m}^2$ , wind speed of 2 m/s, tilt angles of PV panel of  $0^\circ$ ,  $15^\circ$ ,  $30^\circ$  and  $45^\circ$ . The results are shown in Figures 7(a), 7(b), 7(c), and 7(d). The results show that the PV tilt angle has little effect on its operating temperature in both with and without cooling. At different tilt angles, the operating temperature decreases by about 6.8 K (Case 2), 7.4 K (Case 3), 8.2 K (Case 4) compared to without cooling (Case 1). Figure 8 presents the PV efficiency at different tilt angles with and without cooling by heat sink. The results show that the PV conversion efficiency at different tilt angles has very small differences, which is similar to the operating temperature.

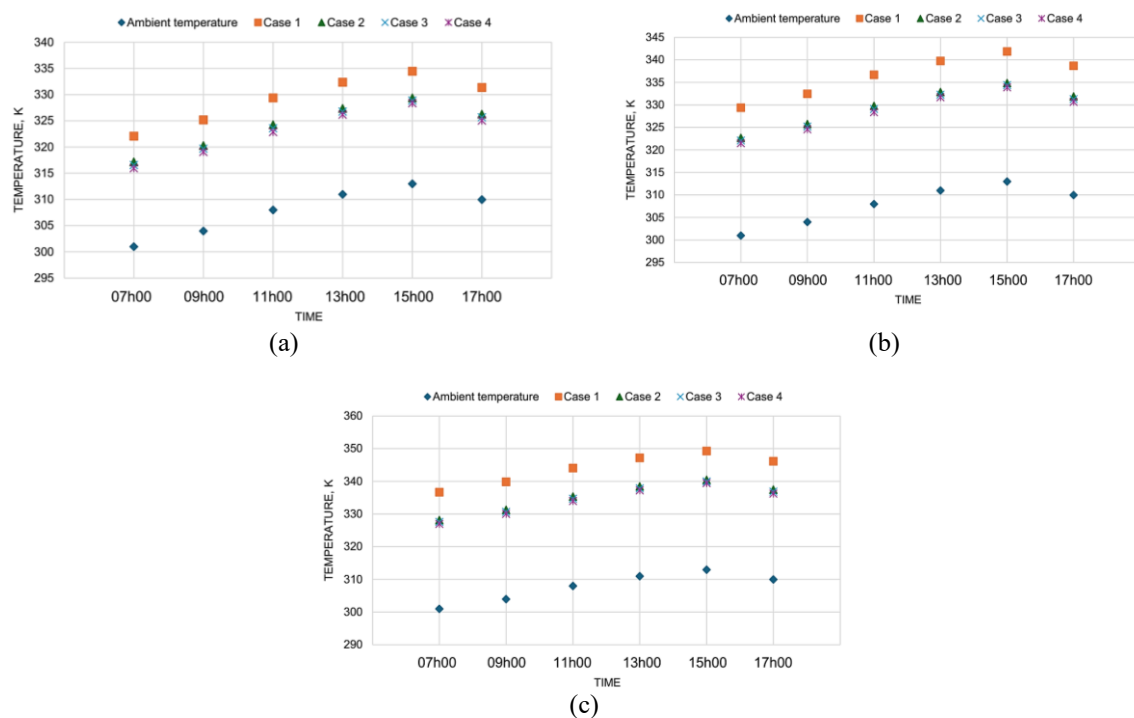


Figure 3. Operating temperature at solar radiation levels: (a)  $600 \text{ W/m}^2$ , (b)  $800 \text{ W/m}^2$ , and (c)  $1000 \text{ W/m}^2$

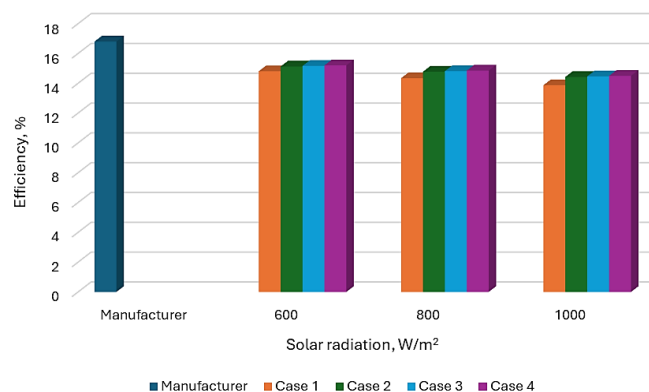


Figure 4. PV efficiency at solar radiation levels



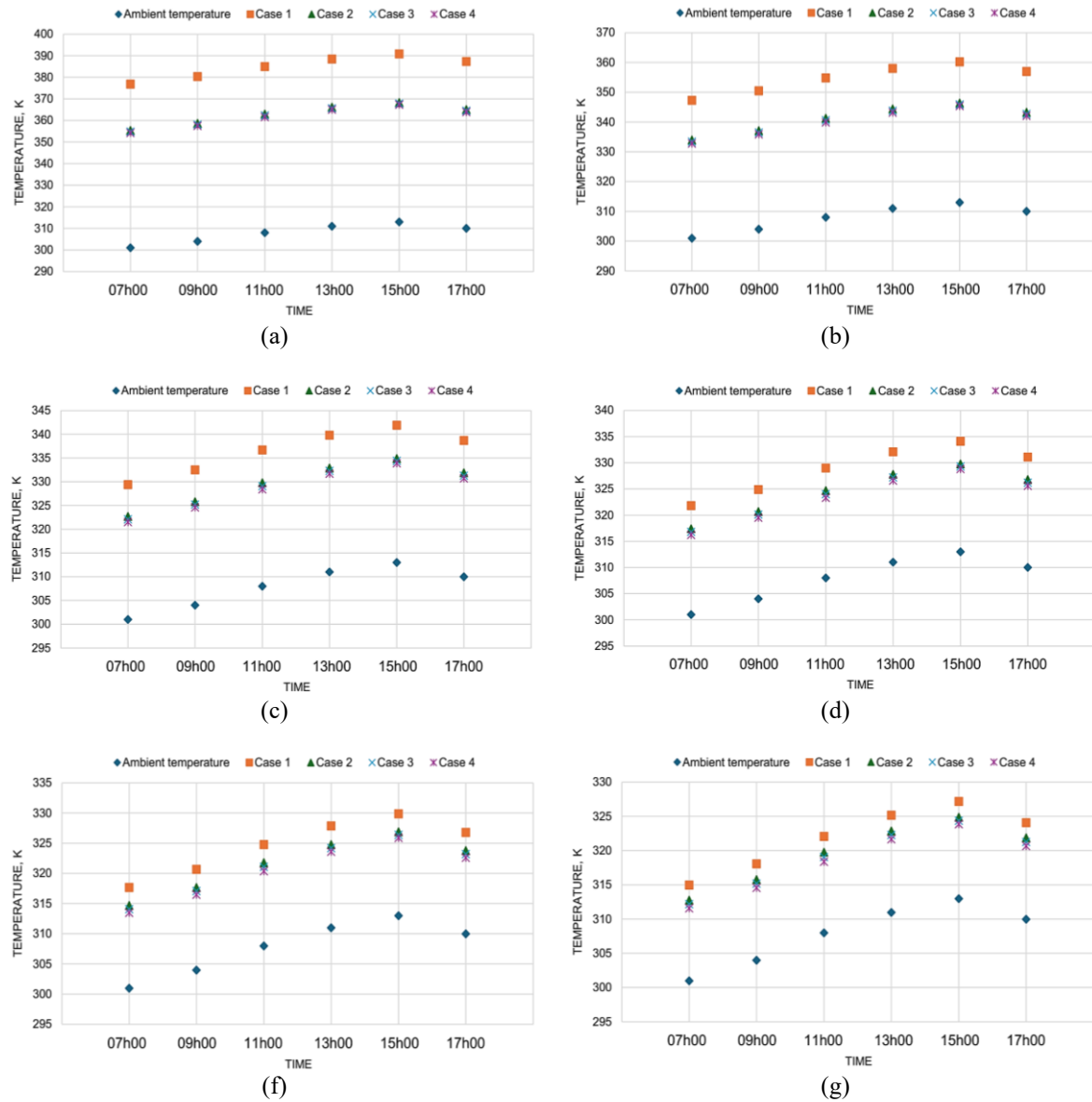


Figure 5. Operating temperature at different wind speeds: (a) 0 m/s, (b) 1 m/s, (c) 2 m/s, (d) 3 m/s, (e) 4 m/s, and (f) 5 m/s

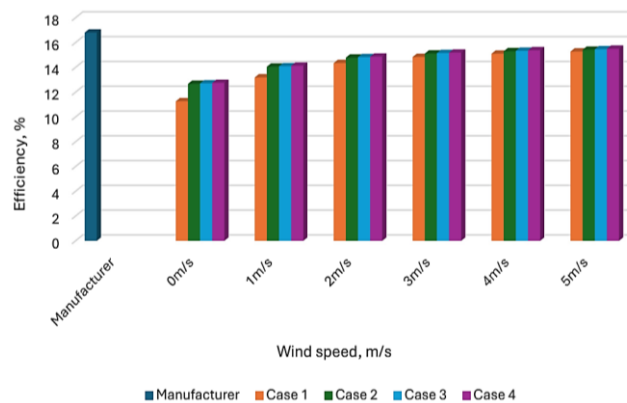


Figure 6. PV efficiency at different wind speeds

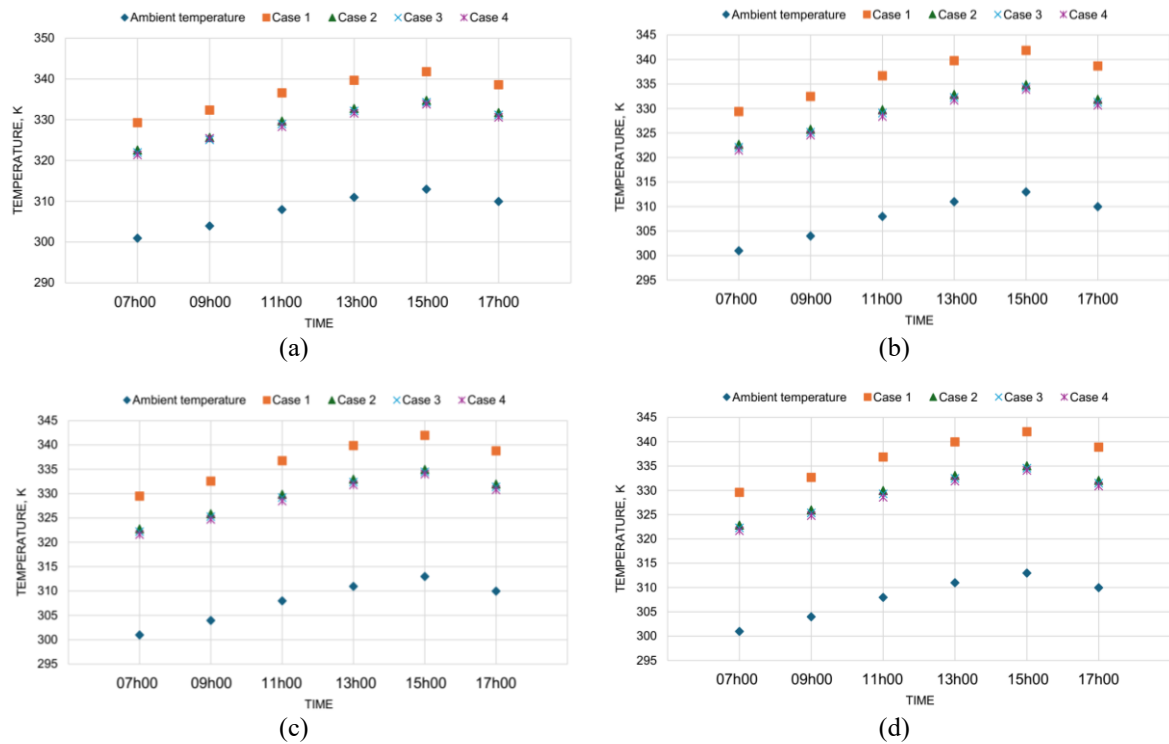


Figure 7. Operating temperature at different tilt angles: (a)  $\theta=0^\circ$ ; (b)  $\theta=15^\circ$ ; (c)  $\theta=30^\circ$ ; and (d)  $\theta=45^\circ$

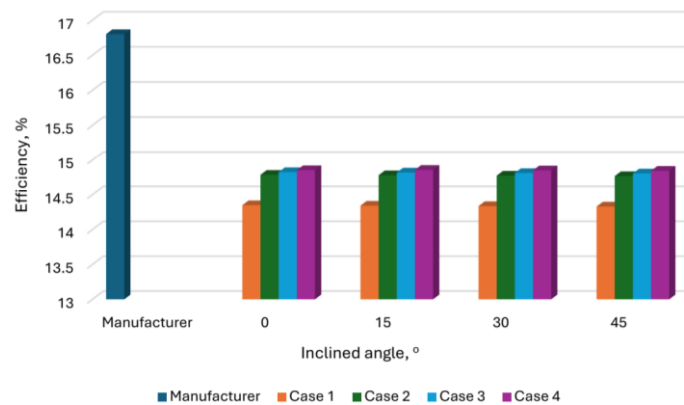


Figure 8. PV efficiency at different tilt angles

## 5. CONCLUSION

The heat sink is a device that helps cool and manage heat for PV panels. Heat sink is added to the back of the PV panel; it increases the ability of convective heat transfer to the environment due to increasing the surface area in contact with the surrounding environment. Heat sink with a base consisting of copper and aluminum layers cool better than aluminum heat sink because the thermal conductivity of copper is better than aluminum. Calculations show that, the PV panel is installed with heat sink, its base has additional copper layer with thickness of 1, 2 mm, the operating temperature of the PV panel is reduced by an average of 0.6 K and 1.2 K compared to the aluminum base. Accordingly, the conversion efficiency of photovoltaic panel increased by 0.1% and 0.2%. In the next study, we will conduct experiments to evaluate the cooling and economic efficiency of the solution in real conditions, and to investigate optimization of heat sink parameters.

## FUNDING INFORMATION

Authors state no funding involved.

## AUTHOR CONTRIBUTIONS STATEMENT

This journal uses the Contributor Roles Taxonomy (CRediT) to recognize individual author contributions, reduce authorship disputes, and facilitate collaboration.

Name of Author	C	M	So	Va	Fo	I	R	D	O	E	Vi	Su	P	Fu
Dang Van Binh	✓	✓	✓		✓	✓	✓	✓	✓		✓			
Pham Quang Vu	✓	✓		✓			✓	✓		✓		✓		
Manh-Hai Pham	✓	✓	✓							✓		✓		

C : Conceptualization

M : Methodology

So : Software

Va : Validation

Fo : Formal analysis

I : Investigation

R : Resources

D : Data Curation

O : Writing - Original Draft

E : Writing - Review & Editing

Vi : Visualization

Su : Supervision

P : Project administration

Fu : Funding acquisition

## CONFLICT OF INTEREST STATEMENT

Authors state no conflict of interest.

## DATA AVAILABILITY

All data used and generated during the analysis in this study are clearly presented within this paper.




## REFERENCES

- [1] A. H. Alami, "Effects of evaporative cooling on efficiency of photovoltaic modules," *Energy Conversion and Management*, vol. 77, pp. 668–679, Jan. 2014, doi: 10.1016/j.enconman.2013.10.019.
- [2] L. W. Thong, S. Murugan, P. K. Ng, and C. C. Sun, "Analysis of photovoltaic panel temperature effects on its efficiency," in *2<sup>nd</sup> International Conference on Electrical Engineering and Electronics Communication System 2016*, 2016, pp. 1–7.
- [3] A. Q. Jakhrani, A. R. Jatoti, and S. H. Jakhrani, "Analysis and fabrication of an active cooling system for reducing photovoltaic module temperature," *Engineering, Technology & Applied Science Research*, vol. 7, no. 5, pp. 1980–1986, Oct. 2017, doi: 10.48084/etasr.1185.
- [4] A. Razak, Y. Irwan, W. Z. Leow, M. Irwanto, I. Safwati, and M. Zhafarina, "Investigation of the effect temperature on photovoltaic (PV) panel output performance," *International Journal on Advanced Science, Engineering and Information Technology*, vol. 6, no. 5, p. 682, Oct. 2016, doi: 10.18517/ijaseit.6.5.938.
- [5] A. U. Chandavar, "Quantifying the performance advantage of using passive solar air heater with chimney for photovoltaic module cooling," *International Journal of Energy Research*, vol. 45, no. 2, pp. 1576–1586, Feb. 2021, doi: 10.1002/er.5782.
- [6] A. Ahmed, K. Shanks, S. Sundaram, and T. K. Mallick, "Theoretical investigation of the temperature limits of an actively cooled high concentration photovoltaic system," *Energies*, vol. 13, no. 8, p. 1902, Apr. 2020, doi: 10.3390/en13081902.
- [7] M. Dida, S. Boughali, D. Bechki, and H. Bouguettaia, "Experimental investigation of a passive cooling system for photovoltaic modules efficiency improvement in hot and arid regions," *Energy Conversion and Management*, vol. 243, p. 114328, Sep. 2021, doi: 10.1016/j.enconman.2021.114328.
- [8] Y. E. Ahmed, M. R. Maghami, J. Pasupuleti, S. H. Danook, and F. Basim Ismail, "Overview of recent solar photovoltaic cooling system approach," *Technologies*, vol. 12, no. 9, p. 171, Sep. 2024, doi: 10.3390/technologies12090171.
- [9] S. Nizetić, A. M. Papadopoulos, and E. Giama, "Comprehensive analysis and general economic-environmental evaluation of cooling techniques for photovoltaic panels, Part I: Passive cooling techniques," *Energy Conversion and Management*, vol. 149, pp. 334–354, Oct. 2017, doi: 10.1016/j.enconman.2017.07.022.
- [10] P. Çulun and S. Kılıçkap Işık, *Chapter 6 recent developments in cooling of photovoltaic solar panels*. 2023.
- [11] J. G. Hernandez-Perez, J. G. Carrillo, A. Bassam, M. Flota-Banuelos, and L. D. Patino-Lopez, "Thermal performance of a discontinuous finned heatsink profile for PV passive cooling," *Applied Thermal Engineering*, vol. 184, p. 116238, Feb. 2021, doi: 10.1016/j.applthermaleng.2020.116238.
- [12] F. Bayrak, H. F. Oztop, and F. Selimefendigil, "Effects of different fin parameters on temperature and efficiency for cooling of photovoltaic panels under natural convection," *Solar Energy*, vol. 188, pp. 484–494, Aug. 2019, doi: 10.1016/j.solener.2019.06.036.
- [13] A. A. Amr, A. A. M. Hassan, M. Abdel-Salam, and A. M. El-Sayed, "Enhancement of photovoltaic system performance via passive cooling: Theory versus experiment," *Renewable Energy*, vol. 140, pp. 88–103, 2019, doi: 10.1016/j.renene.2019.03.048.
- [14] A. H. Shiravi and M. Firoozadeh, "Thermodynamic and environmental assessment of mounting fin at the back surface of photovoltaic panels," *Journal of Applied and Computational Mechanics*, vol. 7, no. 4, pp. 1956–1963, 2021, doi: 10.22055/JACM.2020.32529.2076.
- [15] F. Grubišić-Cabo, S. Nizetić, I. Marinić Kragić, and D. Čoko, "Further progress in the research of fin-based passive cooling technique for the free-standing silicon photovoltaic panels," *International Journal of Energy Research*, vol. 43, no. 8, pp. 3475–3495, Jun. 2019, doi: 10.1002/er.4489.
- [16] Z. Arifin, D. D. D. P. Tjahjana, S. Hadi, R. A. Rachmanto, G. Setyohandoko, and B. Sutanto, "Numerical and experimental investigation of air cooling for photovoltaic panels using aluminum heat sinks," *International Journal of Photoenergy*, vol. 2020, pp. 1–9, Jan. 2020, doi: 10.1155/2020/1574274.
- [17] F. AlAmri, G. AlZohbi, M. AlZahrani, and M. Aboulebdah, "Analytical modeling and optimization of a heat sink design for passive cooling of solar PV panel," *Sustainability*, vol. 13, no. 6, p. 3490, Mar. 2021, doi: 10.3390/su13063490.
- [18] Jorge Andrés Sierra Del Rio *et al.*, "Numerical study of the efficiency of a solar panel with heat sinks," *CFD Letters*, vol. 15, no. 4, pp. 43–52, Feb. 2023, doi: 10.37934/cfdl.15.4.4352.




- [19] J. G. Hernandez-Perez, J. G. Carrillo, A. Bassam, M. Flota-Banuelos, and L. D. Patino-Lopez, "A new passive PV heatsink design to reduce efficiency losses: A computational and experimental evaluation," *Renewable Energy*, vol. 147, pp. 1209–1220, Mar. 2020, doi: 10.1016/j.renene.2019.09.088.
- [20] M. Firoozzadeh, A. Shiravi, and M. Shafiee, "An experimental study on cooling the photovoltaic modules by fins to improve power generation: economic assessment," *Iranian Journal of Energy and Environment*, vol. 10, no. 2, 2019, doi: 10.5829/IJEE.2019.10.02.02.
- [21] A. M. A. Soliman, H. Hassan, and S. Ookawara, "An experimental study of the performance of the solar cell with heat sink cooling system," *Energy Procedia*, vol. 162, pp. 127–135, Apr. 2019, doi: 10.1016/j.egypro.2019.04.014.
- [22] F. Grubišić Čabo, S. Nizetić, E. Giama, and A. Papadopoulos, "Techno-economic and environmental evaluation of passive cooled photovoltaic systems in Mediterranean climate conditions," *Applied Thermal Engineering*, vol. 169, p. 114947, Mar. 2020, doi: 10.1016/j.applthermaleng.2020.114947.
- [23] S. V. Hudişteanu *et al.*, "Effect of wind direction and velocity on PV panels cooling with perforated heat sinks," *Applied Sciences*, vol. 12, no. 19, p. 9665, Sep. 2022, doi: 10.3390/app12199665.
- [24] A. Z. Amri and A. Z. Amri, "Effect of aluminium heat sinks on the temperature reduction and electrical efficiency of monocrystalline solar panels," *European Journal of physical Sciences*, vol. 5, no. 1, pp. 55–65, 2022, doi: 10.47672/ejps.1020.
- [25] E. B. Agyekum, S. PraveenKumar, N. T. Alwan, V. I. Velkin, and S. E. Shcheklein, "Effect of dual surface cooling of solar photovoltaic panel on the efficiency of the module: experimental investigation," *Heliyon*, vol. 7, no. 9, p. e07920, Sep. 2021, doi: 10.1016/j.heliyon.2021.e07920.
- [26] K. P. Amber, W. Akram, M. A. Bashir, M. S. Khan, and A. Kousar, "Experimental performance analysis of two different passive cooling techniques for solar photovoltaic installations," *Journal of Thermal Analysis and Calorimetry*, vol. 143, no. 3, pp. 2355–2366, Feb. 2021, doi: 10.1007/s10973-020-09883-6.
- [27] A. A. Farhan, M. Alaskari, and A. Alhamadani, "A parametric study of a photovoltaic panel with cylindrical fins under still and moving air conditions in Iraq," *Heat Transfer*, vol. 50, no. 1, pp. 596–618, Jan. 2021, doi: 10.1002/htj.21895.
- [28] D. Sundarajan, M. Ganeshkumar, P. Pitchipoo, A. Muthiah, and P. Amuthakannan, "Simulation for enhancing the performance of solar PV module using passive cooling," *IJSTE - International Journal of Science Technology & Engineering*, vol. 7, no. 9, pp. 11–15, 2021.
- [29] P. N. L. Pandiyan, N. G. A. S. and V. V., "Experimental analysis on passive cooling of flat photovoltaic panel with heat sink and wick structure," *Energy Sources, Part A: Recovery, Utilization, and Environmental Effects*, vol. 42, no. 6, pp. 653–663, Mar. 2020, doi: 10.1080/15567036.2019.1588429.
- [30] J. Kim and Y. Nam, "Study on the cooling effect of attached fins on PV using CFD simulation," *Energies*, vol. 12, no. 4, p. 758, Feb. 2019, doi: 10.3390/en12040758.
- [31] K. Egab, A. Okab, H. S. Dywan, and S. K. Oudah, "Enhancing a solar panel cooling system using an air heat sink with different fin configurations," *IOP Conference Series: Materials Science and Engineering*, vol. 671, no. 1, p. 012133, Jan. 2020, doi: 10.1088/1757-899X/671/1/012133.
- [32] S. V. Hudişteanu, F. E. Ţurcanu, N. C. Cherecheş, C. G. Popovici, M. Verdeş, and I. Huditeanu, "Enhancement of PV panel power production by passive cooling using heat sinks with perforated fins," *Applied Sciences*, vol. 11, no. 23, p. 11323, Nov. 2021, doi: 10.3390/app112311323.
- [33] Z. Arifin, S. Suyitno, D. D. P. Tjahjana, W. E. Juwana, M. R. A. Putra, and A. R. Prabowo, "The effect of heat sink properties on solar cell cooling systems," *Applied Sciences*, vol. 10, no. 21, p. 7919, Nov. 2020, doi: 10.3390/app10217919.
- [34] S.-V. Hudişteanu, N.-C. Cherecheş, F.-E. Ţurcanu, I. Hudişteanu, M. Verdeş, and A.-D. Ancaş, "Experimental analysis of innovative perforated heat sinks for enhanced photovoltaic efficiency," *Energy Conversion and Management: X*, vol. 25, p. 100842, Jan. 2025, doi: 10.1016/j.ecmx.2024.100842.
- [35] D. Van Binh *et al.*, "Passive cooling for photovoltaic using heat sinks: a recent research review," in *2023 Asia Meeting on Environment and Electrical Engineering (EEE-AM)*, Nov. 2023, pp. 01–06, doi: 10.1109/EEE-AM58328.2023.10395427.
- [36] Y. A. Çengel, *Heat and Mass Transfer: Fundamentals and Applications*, 5<sup>th</sup> ed. New York, NY, USA: McGraw-Hill, 2014.
- [37] F. P. Incropera and D. P. DeWitt, *Fundamentals of Heat and Mass Transfer*, 4<sup>th</sup> ed. New York, NY, USA: Wiley, 1996.
- [38] E. Sartori, "Convection coefficient equations for forced air flow over flat surfaces," *Solar Energy*, vol. 80, no. 9, pp. 1063–1071, Sep. 2006, doi: 10.1016/j.solener.2005.11.001.
- [39] T. Fujii and H. Imura, "Natural-convection heat transfer from a plate with arbitrary inclination," *International Journal of Heat and Mass Transfer*, vol. 15, no. 4, pp. 755–767, Apr. 1972, doi: 10.1016/0017-9310(72)90118-4.
- [40] Y. Abudllah, Z. Arifin, D. Danardono Dwi Prija Tjahjana, S. Suyitno, and M. R. Aulia Putra, "Analysis of the copper and aluminum heat sinks addition to the performance of photovoltaic panels with CFD modelling," in *2020 1<sup>st</sup> International Conference on Information Technology, Advanced Mechanical and Electrical Engineering (ICITAMEE)*, Oct. 2020, pp. 41–45, doi: 10.1109/ICITAMEE50454.2020.9398314.

## BIOGRAPHIES OF AUTHORS






**Dang Van Binh**    received bachelor's degree in thermal engineering from University of Transport and Communications, Hanoi, Vietnam in 2009 and master degree in energy engineering from Electric Power University, Hanoi, Vietnam in 2017. Currently, he is a lecturer at Hanoi University of Industry, Hanoi, Vietnam and a Ph.D. student at Electric Power University, Hanoi, Vietnam. His research interests include thermal engineering, energy engineering, saving energy, heat transfer, renewable energy. He can be contacted at email: binhdv@hau.edu.vn.



**Pham Quang Vu**    received bachelor's degree from School of Biotechnology and Food Technology, Hanoi University of Science and Technology, Hanoi, Vietnam in 2011 and Ph.D. degree in refrigeration and air-conditioning engineering from Chonnam National University, Gwangju, South Korea in 2019. Currently, he is a lecturer at Electric Power University, Hanoi, Vietnam. His research interests include thermal engineering, energy engineering, saving energy, heat transfer, refrigeration and air-conditioning engineering. He can be contacted at email: vupq@epu.edu.vn.



**Manh-Hai Pham**    received bachelor's degree in electrical engineering from Hanoi University of Science and Technology, Hanoi, Vietnam in 2006, master degree in electrical engineering from Paul Sabatier University, Toulouse, France in 2008, and Ph.D. degree in applied organic chemistry - Plasma for energy at Poitiers University (ENSIP), Poitiers, France in 2011. Currently, he is a lecturer at Electric Power University, Hanoi, Vietnam. His research interests include optimization algorithms, electricity load forecasting, artificial intelligence algorithms, wind and solar power forecasting, renewable energy, biomass-biogas production, reliability in the system electrical system. He can be contacted at email: haipm@epu.edu.vn.